# Magnetization-reversal mechanism of hard/soft exchange-coupled trilayers

Shi-shen Yan,* W. J. Liu, J. L. Weston, G. Zangari, and J. A. Barnard
*Center for Materials for Information Technology, The University of Alabama, Tuscaloosa, Alabama 35487-0209*
(Received 21 August 2000; revised manuscript received 27 November 2000; published 5 April 2001)

$Ni_{80}Fe_{20}/Sm_{40}Fe_{60}/Ni_{80}Fe_{20}$ trilayers with in-plane uniaxial anisotropy induced by an applied magnetic field during deposition were prepared on (100)-Si substrates by dc magnetron sputtering. Magnetization hysteresis loops were measured by an alternating-gradient magnetometer for various angles between the external magnetic field and the easy axis. The experimental hysteresis loops were quantitatively described by a theoretical model that combines coherent rotation and domain-wall unpinning. When the external field is along the easy axis, the magnetization reversal is caused by domain-wall unpinning. When the external field is along or near the hard axis, the magnetization reversal is caused by coherent rotation. For other orientations, the magnetization first rotates gradually by coherent rotation and then sharply switches by domain-wall unpinning. The domain-wall angle and the pinning energy at the sharp switching strongly depend on the angle between the external field and the easy axis. Furthermore, the dependence of the coercivity measured in the easy direction on the thickness of $Ni_{80}Fe_{20}$ layers was theoretically reproduced by an extended model of domain-wall unpinning.

DOI: 10.1103/PhysRevB.63.174415 PACS number(s): 75.60.Ej, 75.70.−i

## I. INTRODUCTION

One of the controversial issues in the study of magnetic materials has been the mechanism of magnetic reversal.[1] For permanent magnets such as bulk $Nd_2Fe_{14}B$ and $Sm_2Co_{17}B$, in order to explain the reduced coercivity due to inhomogeneities such as grain boundaries, inclusions, or defects in the main magnet phase, an empirical form for the coercive field was proposed as follows,[1]

$$H_C(T)=\alpha(T)2K_1/M_s-N_{\text{eff}}M_s, \tag{1}$$

where $\alpha(T)$ corresponds to a microstructural parameter and $N_{\text{eff}}$ to an averaged local effective demagnetization factor. Although in some cases Eq. (1) gives a fair description of the experimental coercivity, it is difficult to distinguish the pinning and nucleation according to Eq. (1) because both domain-wall pinning at the inhomogeneities and nucleation of reversed domains in the same region lead to the same expression. In fact, neither the pinning model nor the nucleation model fully explain the experimental results. In particular, the dependence of the coercivity on the angle between the external field and the easy axis is poorly described.

From the viewpoint of micromagnetic theory, although the pinning and nucleation models have the same physical picture of microstructural defects, their conclusions about coercivity are quite different and even contradictory.[2–4] However, it is difficult to directly compare the experimental results with the micromagnetic calculation because the microstructural parameters of a real system are often poorly known. On the other hand, in the case of real magnets that often have misaligned grains, neither the pinning coercivity nor the nucleation coercivity as determined for an ideally oriented magnet can correctly describe the orientation dependence of the measured coercivity.

For single-crystal soft magnetic thin films, there also exists a similar controversy about pinning and nucleation.[5–8] Our recent study of the magnetization reversal of (001)-oriented single-crystal Fe films with fourfold in-plane anisotropy indicates that in a hysteresis loop gradual reversal is caused by coherent rotation, and sharp switching is caused by domain-wall unpinning.[5] It is an open question as to whether the two-path reversal mechanism can apply to other magnetic systems with well-defined uniaxial anisotropy.

Synthetic magnetic materials consisting of hard- and soft-magnetic phases that couple together through direct exchange interaction can be designed to have a giant energy product for permanent magnets[9,10] or a giant magnetostriction at relatively low field.[11] The realization of these properties is also related to the magnetization-reversal process. Since most theoretical models of magnetic reversal are based on the same microstructure, i.e., soft-magnetic inhomogeneities are embedded in the main magnet phase, hard/soft exchange-coupled magnetic multilayers, that are composed of alternating hard- and soft-magnetic layers of controllable thickness supply a simple but realistic model system for the study of the mechanism of magnetic reversal. For sufficiently thin soft-magnetic layers (of the order of a domain-wall width in the hard layers) that are supposed to be rigidly coupled to the hard layers, the whole multilayer will switch at a nucleation field given by[12]

$$H_N=2(t_hK_h+t_sK_s)/(t_hM_h+t_sM_s), \tag{2}$$

where $t_h$ ($t_s$), $K_h$ ($K_s$), and $M_h$ ($M_s$) are the thickness, anisotropy, and magnetization of the hard (soft) layers, respectively. However, such behavior was only shown qualitatively in magnetic multilayers, such as SmCo/FeCo bilayers[13] and NdFeB/Fe superlattices.[14] On the other hand, for thick soft-magnetic layers, the exchange spring behavior[12,15–17] occurs during the process of the magnetization reversal.

In the present paper, we consider the $Ni_{80}Fe_{20}/Sm_{40}Fe_{60}/Ni_{80}Fe_{20}$ trilayers where soft NiFe layers and hard SmFe layers rigidly couple together and show a well-defined in-plane uniaxial anisotropy. The whole process of the magnetic reversal in this ideal system was experimentally studied through hysteresis loops. We determined

 

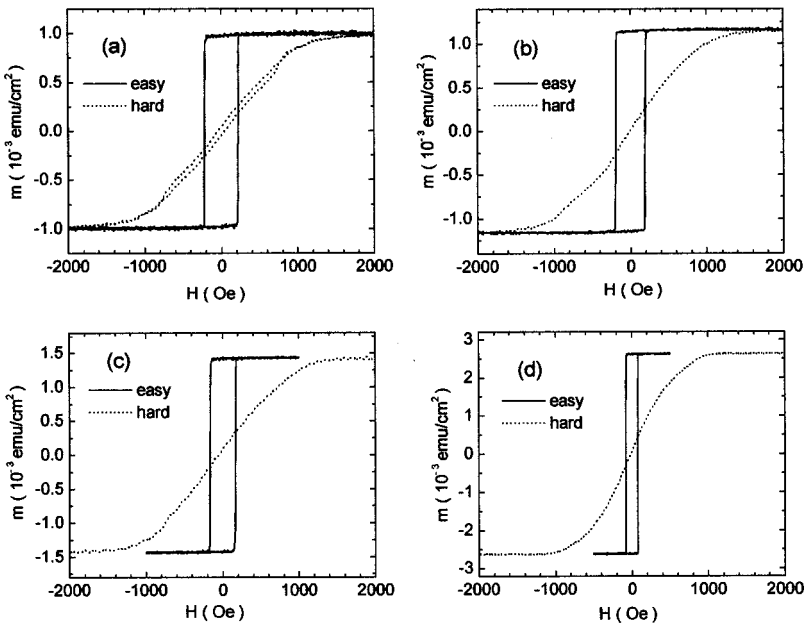


FIG. 1. Typical magnetization hysteresis loops of NiFe/SmFe/NiFe trilayers measured in the easy- and hard-axis directions. The thickness of the SmFe layer is fixed at 14.6 nm. The thickness of the NiFe layers is, respectively, (a) 3.1, (b) 4.7, (c) 6.2, and (d) 12.5 nm.

whether the experimental hysteresis loops could be quantitatively described by a theoretical model that combines coherent rotation and domain-wall unpinning.[5] Furthermore, the thickness dependence of the coercivity in the easy direction was explained by an extended model of domain-wall unpinning.

## II. EXPERIMENTS

$Ni_{80}Fe_{20}/Sm_{40}Fe_{60}/Ni_{80}Fe_{20}$ trilayers of various thickness were prepared on (100)-Si substrates by dc magnetron sputtering at room temperature. The pressure of Ar gas was stabilized at 3 or 5 mTorr during the sputtering process. Unless specified, an Ar pressure of 3 mTorr was used. The deposition rates for NiFe and SmFe layers are, respectively, 0.15 and 0.16 nm/s. In order to get an in-plane uniaxial anisotropy induced in the direction of the external field, two permanent magnets were used to supply an external magnetic field of 80 Oe in the film plane during growth. A 5-nm $Si_3N_4$ protective layer was deposited on the top of the samples by rf sputtering *in situ*. The structural properties of the NiFe/SmFe/NiFe trilayers were characterized by low- and high-angle x-ray diffraction. The low-angle x-ray-diffraction patterns indicate that the NiFe/SmFe/NiFe trilayers have a good layered structure. The high-angle x-ray-diffraction patterns indicate that NiFe layers exhibit fcc (111) crystalline texture and the SmFe layer is in an amorphous state. The magnetization hysteresis loops were measured by alternating-gradient magnetometer (AGM) for various angles between the external magnetic field and the easy axis. All the experimental results were measured at room temperature.

## III. EXPERIMENTAL RESULTS AND THEORETICAL MODEL

Figures 1(a)–1(d) show typical magnetization hysteresis loops measured along the easy and hard axes. When the external field is along the easy direction, the hysteresis loops (easy-axis hysteresis loops) are nearly perfectly rectangular, as shown in Figs. 1(a)–1(d) (solid lines). When the external field is along the hard direction, the hysteresis loops with very small hysteresis and even no hysteresis (hard-axis hysteresis loops) almost become oblique lines for thin NiFe layers, as shown in Figs. 1(a)–1(c) (dotted lines). This indicates that the samples have a well-defined in-plane uniaxial anisotropy for thin NiFe layers that is induced by the external field during deposition. As the thickness of NiFe layers further increases, the hard-axis loops begin to deviate from the oblique lines, as shown in Fig. 1(d) (dotted line). However, the easy-axis loops are still rectangular, as shown in Fig. 1(d) (solid line). With increasing NiFe thickness, although the magnetization of NiFe and SmFe layers still reverses together when the field is along the easy direction, the magnetization of NiFe and SmFe layers has begun to rotate incoherently when the field is along the hard direction.

In order to study the mechanism of magnetic reversal, hysteresis loops were measured by AGM for various angles $\phi_H$ between the external field and the easy axis (both the external field and the easy axis are in the film plane). In this case, it is possible to understand the whole process of the magnetization reversal. Figures 2(a)–2(d) show typical hysteresis loops for NiFe 2.4/SmFe 13/NiFe 2.4 nm trilayers measured at different $\phi_H$. The hysteresis loops only show one sharp jump at which the magnetic reversal is irreversible (the field at the jump is the switching field). At first glance, these loops are characteristic of uniaxial anisotropy materials. However, even in so simple a case, the switching field at different $\phi_H$ cannot be quantitatively described by the conventional coherent rotation or domain-wall unpinning models.

For a quantitative description of the experimental hysteresis loops, a theoretical model (two-path reversal model) proposed in Ref. 5 was extended to apply to the present case. Here we first introduce this model to the present system.

For thin NiFe layers, NiFe and SmFe strongly couple to-

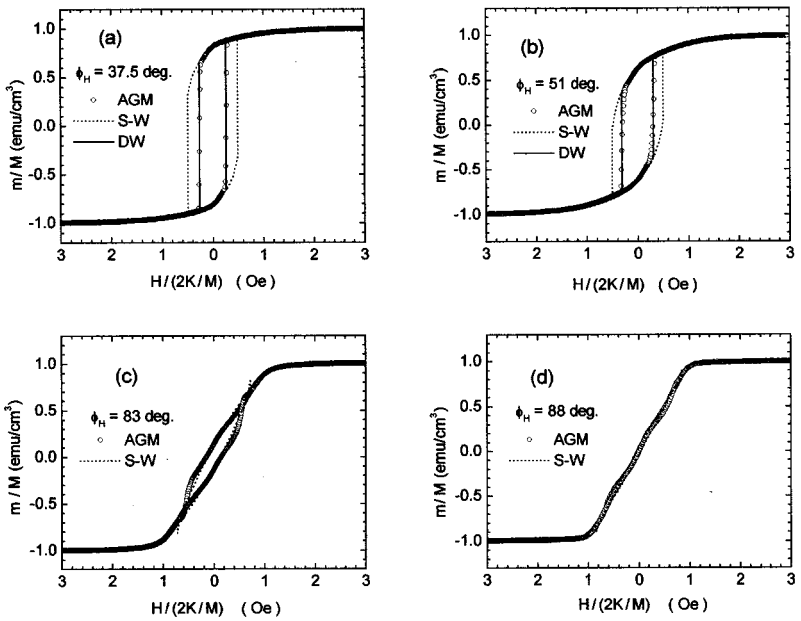


FIG. 2. (a)–(d). Typical hysteresis loops measured at different angles $\phi_H$ (circles) and theoretical results according to the Stoner-Wohlfarth (SW) model (dotted lines) and the two-path reversal model (solid lines). For simplicity, the reduced values of magnetization (divided by the averaged value of saturation magnetization of the sample $M=440$ emu/cm$^3$) and external field (divided by the value of the anisotropy field $H_K=2K/M=529$ Oe) are used in the calculation. The thickness of the trilayers is, respectively, NiFe 2.4/SmFe 13/NiFe 2.4 nm, and the sample was prepared at 5 mTorr Ar gas.

gether, so the magnetic reversal in different layers occurs together, behaving like a homogeneous single film. It is reasonable to suppose that all magnetic domains are always located in the states of local minimum energy and the total-energy per unit volume in any domain can be written as follows:

$$E(H,\phi_M)=-HM\cos(\phi_M-\phi_H)+K\sin^2(\phi_M), \quad (3)$$

where $K$, $M$, and $H$ are, respectively, the effective in-plane uniaxial anisotropy, the averaged saturation magnetization, and the applied external field; $\phi_M$ is the angle between the magnetization vector and the easy axis; and $\phi_H$ is the angle between the positive direction of the applied field and the easy axis. Now suppose that the whole sample, except the edges of the sample and a few defects, is in a single-domain state determined by the local minimum energy of Eq. (3). Denote this domain as the main domain and its energy state as $E_1(H,\phi_{M1})$. The magnetization $m(H)$ of the hysteresis loop is determined by the main domain and

$$m(H)=M\cos(\phi_{M1}-\phi_H). \quad (4)$$

On the other hand, it is also supposed that there exist simultaneously a few very small domains near the sample edges or defects. We denote the very small domains as minor domains and their energy state as $E_2(H,\phi_{M2})$. The minor domains are assumed to have the same magnetic parameters ($M$, $K$, and the exchange constant $A$) as those of the main domain and their energy state $E_2(H,\phi_{M2})$ is also determined by the local minimum energy of Eq. (3). So $E_1(H,\phi_{M1})$ and $E_2(H,\phi_{M2})$ may be the two states of different local minimum energy at the same external field. The domain wall between the main and minor domains is pinned at a defect region (its magnetic parameters may be different from those of the soft and hard layers) and the pinning energy density is $\varepsilon(H)$. On increasing the strength of the reverse field to a certain value, the following equation may be established,

$$E_1(H,\phi_{M1})-E_2(H,\phi_{M2})\geqslant\varepsilon(H). \quad (5)$$

In this case, the domain wall will become unstable and the magnetization reverses sharply by domain-wall unpinning. This field is defined as the switching field $H_S$, $\varepsilon(H_S)$ as the unpinning energy of the domain wall, and $\Delta\phi=|\phi_{M1}-\phi_{M2}|$ as the domain-wall angle at the switching field. On the other hand, if Eq. (5) never has a real solution for a given cycle of the external field, domain-wall unpinning will never occur. So, in this case the magnetic reversal is completely determined by Eq. (3), which comes back to the prediction of the Stoner-Wohlfarth (SW) coherent rotation model.

As for Eq. (5), if the rotation of the magnetization in the field is neglected, which is otherwise determined by the local minimum energy of Eq. (3), $\phi_{M1}$, $\phi_{M2}$, and $\varepsilon(H)$ can be regarded as constants; for example, $\phi_{M1}=0$, $\phi_{M2}=\pi$, and $\varepsilon(H)=\varepsilon_0$. For the external field $H$ oriented at $\phi_H=\theta$, according to Eqs. (3) and (5), $2H_SM\cos(\theta)=\varepsilon_0$ can be obtained at the switching field $H_S$, i.e., $H_S=\varepsilon_0/[2M\cos(\theta)]$. In this case Eq. (5) becomes the conventional domain-wall unpinning model.

In the above two-path reversal model, the activation energy may be involved in establishing the domain walls. Since this happens at inhomogeneities and is clearly not a limiting step, the thermal activation process is ignored in Eqs. (3)–(5). Only the driving energy needed to unpin the domain walls is considered so that they propagate freely across the whole sample. Moreover, the minor domain often exists at the edges of the sample, and the edges are generally too small to observe by magnetooptic Kerr microscopy except at the switching field.[5] Only at the switching field do some minor domains grow large quickly and sweep through the whole sample, replacing the main domain.

For any given NiFe/SmFe/NiFe trilayer, $K$ and $M$ are constants ($M$ can be measured by AGM, and $H_K=2K/M$ is equal to the saturation field in the hard direction), so for any given $\phi_H$, if $\varepsilon(H)$ is known the whole hysteresis loop can be calculated according to Eqs. (3)–(5). However, in the

present case, $\varepsilon(H)$ is not known in advance. The value of $\varepsilon(H)$ depends on the details of the defects (such as the size, magnetization, anisotropy, and exchange constant) and the magnetic parameters of the soft and hard layers. A micromagnetic calculation is needed to determine $\varepsilon(H)$, but this is not the object of the present paper. Here the theoretical model is fitted to the experimental hysteresis loops to get information about $\varepsilon(H)$. Specifically, the theoretical model is fitted to an experimental hysteresis loop in the whole range of the field except at the point of the switching field. At the switching field $H_S$, the fitting is terminated at the two ends of the sharp jump that correspond to the two states of the local minimum energies $E_1(H_S,\phi_{M1})$ and $E_2(H_S,\phi_{M2})$ of Eq. (3). Then the unpinning energy of the domain wall $\varepsilon(H_S)$ and the domain-wall angle $\Delta\phi$ at the switching field according to Eq. (5) can be given as follows,

$$\varepsilon(H_S)=E_1(H_S,\phi_{M1})-E_2(H_S,\phi_{M2}), \tag{6}$$

$$\Delta\phi=|\phi_{M1}-\phi_{M2}|. \tag{7}$$

Figure 2 shows the theoretical fitting (solid lines) to the experimental hysteresis loops (circles) according to the two-path reversal model. As a comparison, the theoretical results of the SW model [only according to Eq. (3)] are also shown (dotted line) in Fig. 2. Figures 2(c) and 2(d) indicate that the experimental hysteresis loops are in good agreement with the theoretical prediction of the SW model when the external field is near the hard direction. This indicates that the whole process of the magnetic reversal is completely determined by coherent rotation. In this case, the energy difference between the main and the minor domains is very small and always less than the pinning energy of the domain wall, so the unpinning of the domain wall will never occur. However, when the external field is far away from the hard direction, the theoretical predictions of the SW model are no longer in agreement with the experimental hysteresis loops, as shown in Figs. 2(a) and 2(b). According to the two-path reversal model, the coherent rotation process was terminated at the switching field and the domain-wall unpinning process occurs, as shown by the solid lines in Figs. 2(a) and 2(b). After the sharp jump caused by the domain-wall unpinning, the magnetization continues to reverse by coherent rotation until saturation.

Figure 3 shows the experimental switching field $H_S$ (triangles) and the coercivity $H_C$ (circles) at various angles $\phi_H$ as well as the theoretical switching field of the SW model (solid line). Here the switching field $H_S$ is the field at which the irreversible magnetic reversal (at the sharp jump of the hysteresis loop) occurs, and the coercivity $H_C$ is defined as the field at which the magnetization on a hysteresis loop is zero. According to the definition, the magnetic reversal is characterized by the switching field, not by the coercivity. Figure 3 shows $H_S=H_C$ when $\phi_H<51°$. In this case, the coercivity can be used to characterize the magnetic reversal. In the other cases, the coercivity is different from the switching field. Figure 3 also shows that the experimental switching field is in good agreement with the prediction of the SW model when $\phi_H>76°$. So in this case the magnetic reversal

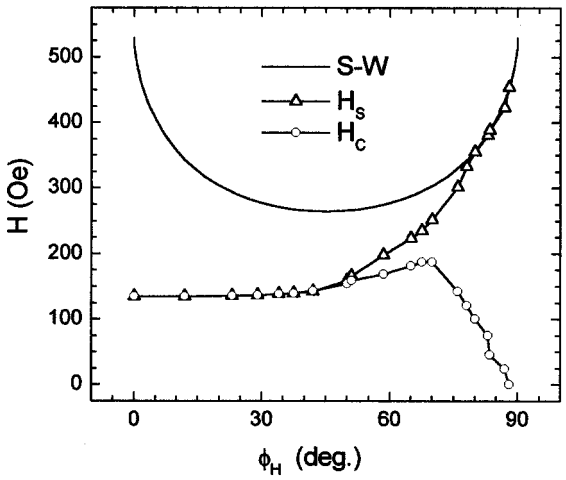


FIG. 3. The experimental switching field $H_S$ (triangles) and the coercivity $H_C$ (circles) at various angles $\phi_H$, as well as the theoretical switching field (solid line) of the SW model. Some hysteresis loops of this sample have been shown in Figs. 2(a)–(d).

is completely determined by coherent rotation, instead of domain-wall unpinning, which becomes important when $\phi_H<76°$.

Figure 4 shows the $\phi_H$ dependence of the domain-wall angle and the unpinning energy at the switching field. In Fig. 4, the domain-wall angle and the unpinning energy are not constants, but gradually reduce when $\phi_H$ increases. It is well known that the domain-wall angle and the unpinning energy are assumed to be constants in the conventional model of domain-wall unpinning. Figure 4 shows that the domain-wall

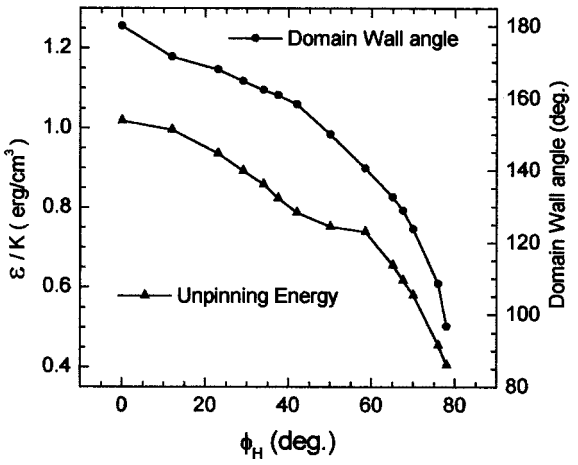


FIG. 4. The $\phi_H$ dependence of the domain-wall angle $\Delta\phi$ and the unpinning energy density $\varepsilon(H_S)$ at the switching field for the same sample shown in Figs. 2 and 3. For simplicity, the reduced values of pinning energy density (divided by the value of anisotropy $K=1.164\times10^5$ erg/cm$^3$) and external field (divided by the value of the anisotropy field $H_K=2K/M=529$ Oe) are used in the calculation. For any given sample, $K$ and $M$ are certain constants. Using the reduced values, Eq. (3) becomes more universal so that fitting Eq. (3) to the experimental hysteresis loops is possible if the value of $H_K=2K/M$ is known, instead of both $M$ and $K$.

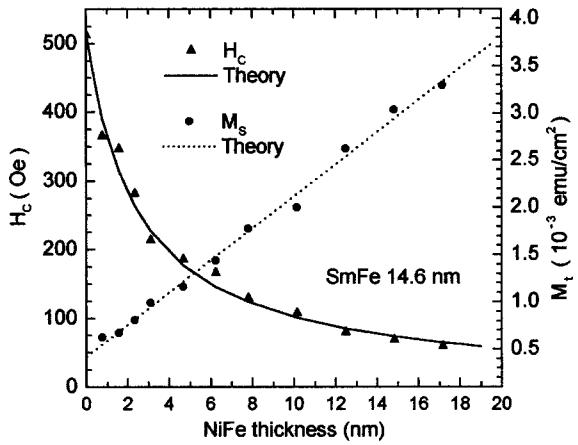


FIG. 5. The dependence of the easy-axis coercivity and the magnetization per unit area on the thickness of the NiFe layer. The thickness of the SmFe layer is fixed at 14.6 nm. The triangles present the experimental coercivity, and the solid line presents the theoretical prediction of Eq. (11). The circles present the experimental magnetization per unit area and the dotted line presents the theoretical prediction of Eq. (12).

angle is 180° and the unpinning energy is maximum when the external field is along the easy axis ($\phi_H=0$). In this case, the two-path model and the conventional unpinning model give the same results. However, when the reversal field is not along the easy direction, the magnetization vector in any domain will deviate from the easy direction and rotate toward the direction of the reversal field until the domain wall unpins. So, in this case the domain-wall angle reduces and correspondingly the pinning energy exerted on the domain wall is reduced.

The two-path model is further checked by studying the dependence of the coercivity measured in the easy direction (easy-axis coercivity) on the thickness of the hard and soft layers. Figure 5 (triangles) shows the NiFe thickness dependence of the easy-axis coercivity. In this series of samples, the SmFe thickness is fixed at 14.6 nm, and the NiFe thickness is systematically changed. In Fig. 5, the coercivity first reduces quickly and then reduces slowly as the thickness of the NiFe layers increases. A similar phenomenon has been observed by other researchers,[12,13] but a sound quantitative explanation is still lacking. We have known from the above that for the strongly exchange-coupled trilayers the easy-axis hysteresis loops are nearly perfectly rectangular and the coercivity is caused completely by domain-wall unpinning. In this case the two-path model automatically reduces to the conventional model of domain-wall unpinning, so the conventional model of domain-wall unpinning is directly extended to describe the dependence of the easy-axis coercivity on the thickness of hard and soft layers. Assuming that the pinning energy density exerted on the domain walls is, respectively, $\varepsilon_h$ and $\varepsilon_s$ in the SmFe hard layer and the two NiFe soft layers, the averaged or effective pinning energy density $\varepsilon$ is given by Eq. (8) as

$$\varepsilon=(t_h\varepsilon_h+2t_s\varepsilon_s)/(t_h+2t_s), \tag{8}$$

and the averaged saturation magnetization is given by Eq. (9) as follows:

$$M=(t_hM_h+2t_sM_s)/(t_h+2t_s). \tag{9}$$

So the easy-axis coercivity determined by the unpinning mechanism can be formulated as

$$H_C=\varepsilon/2M=(t_h\varepsilon_h+2t_s\varepsilon_s)/(t_hM_h+2t_sM_s)/2. \tag{10}$$

Since the coercivity (or $\varepsilon_h$) of a SmFe single film (a few hundred oersted) is much bigger than that of a NiFe single film (<2 Oe) in our case, the term $2t_s\varepsilon_s$ can be neglected as compared with the term $t_h\varepsilon_h$, and Eq. (10) becomes Eq. (11).

$$\begin{aligned}H_C=\varepsilon/2M&\cong(\varepsilon_h/2M_h)t_h/[t_h+(M_s/M_h)2t_s]\\&=H_0t_h/(t_h+2\alpha t_s),\end{aligned} \tag{11}$$

where $H_0=\varepsilon_h/2M_h$ can be regarded as the coercivity of a single SmFe film ($H_0$ may depend on the thickness of the SmFe layer), and $\alpha=M_s/M_h$ is the ratio (constant) of the magnetization of the NiFe layer to that of the SmFe layer. For fixed SmFe thickness $t_h$, $H_0$ is a constant in Eq. (11), so only the FeNi thickness $t_s$ is a variable. In Fig. 5 (solid line) the coercivity calculated according to Eq. (11) is shown. In the calculation, the following experimental constants are used. $M_s=856$, $M_h=286\,\mathrm{emu/cm^3}$, $H_0=512\,\mathrm{Oe}$, and $t_h=14.6\,\mathrm{nm}$. Fig. 5 shows that the experimental coercivity is well reproduced by the extended domain-wall unpinning model in terms of Eq. (11).

For exchange-coupled hard/soft trilayers, the total magnetic moments are equal to the sum of the magnetic moments in all layers. So the magnetization per unit area $M_t$ can be given as follows:

$$M_t=(t_hM_h+2t_sM_s). \tag{12}$$

Figure 5 (circles) shows the experimental magnetization per unit area and the theoretical expectations (dotted line) according to Eq. (12). It is clear that the experimental results are in good agreement with the theoretical expectations. This indicates that the modulated thickness in the trilayers is highly controllable, which makes a systematic and quantitative study of the mechanism of the coercivity possible.

In addition, magnetic properties were systematically studied by varying the thickness of the hard layer while fixing the thickness of the soft layers. Figure 6 shows the SmFe thickness dependence of the easy-axis coercivity and the magnetization per unit area. For this series of samples, the pressure of Ar gas is stabilized at 5 mTorr, the thickness of each NiFe layer is fixed at 2.6 nm, and the thickness of the SmFe layers is systematically changed. In Fig. 6 (triangles), the coercivity gradually increases with increasing thickness of the SmFe layer, a similar dependence to that observed by others.[13] The magnetization per unit area is also shown in Fig. 6 (circles), which is in good agreement with the theoretical expectations (dotted line) according to Eq. (12). However, because the coercivity $H_0$ (or $\varepsilon_h$) depends on the thickness of the hard layer, the SmFe thickness dependence of the

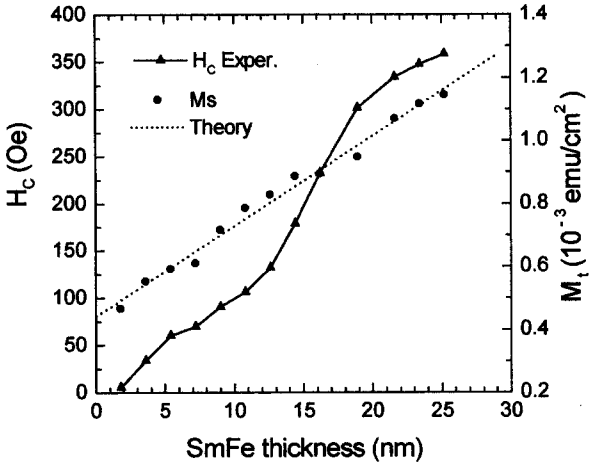


FIG. 6. The SmFe thickness dependence of the easy-axis coercivity (triangles) and the magnetization per unit area (circles). The dotted line presents the theoretical prediction of magnetization per unit area by Eq. (12). The thickness of the NiFe layer is fixed at 2.6 nm and the sputtering pressure of Ar gas is kept at 5 mTorr.

coercivity of the trilayers cannot be calculated by using a constant $H_0$ in Eq. (11), though Eq. (11) is still effective. It was also found that the coercivity is sensitive to the sputtering Ar gas pressure but the magnetization of hard and soft layers almost does not change when the Ar gas pressure changes from 3 to 5 mTorr.

## IV. DISCUSSION

The basic idea of the two-path reversal mechanism has been proposed, implied or supported by other researchers.[5,6,18] The quantitative two-path reversal model was first applied to single-crystal Fe films with fourfold in-plane anisotropy.[5] In this paper the model was extended to apply to an exchange-coupled multilayered system with a well-defined in-plane uniaxial anisotropy. In epitaxial $CrO_2$ thin films with in-plane uniaxial anisotropy, a similar reversal model was used to explain the experimental results.[18] The authors used the conventional coherent rotation model to describe the whole hysteresis loop except at the switching field, but used the conventional domain-wall unpinning model to describe the switching field. Since the conventional coherent rotation model and domain-wall unpinning model are not compatible in the same physics picture, the switching field can be approximately described only for the case that the external field is far away from the hard axis. However, all these results strongly support the two-path reversal model.

For hard/soft exchange-coupled multilayers, even though the microstructural and the magnetic parameters can be regarded as homogeneous in layers of the same composition, they are quite different in layers of different compositions. In this sense hard/soft exchange-coupled multilayers are highly inhomogeneous systems. However, owing to the strong exchange coupling, the systems still exhibit the macromagnetic properties of a homogeneous system if the soft layers are not too thick. This greatly simplifies the theoretical model of magnetic reversal. In fact, even in each soft or hard layer, there still exists some defects that show different magnetic parameters from those of the soft and hard layers. Since the soft and hard layers cannot show their independent magnetization behavior in the hysteresis loops in the strong-coupling case, we cannot expect that the small defects inside the layers can show their own magnetization behavior independently. So in our simple model we need not consider the details of the defects. In this case, the whole trilayer, at least in the scale of the exchange length, will show its magnetization behavior like a single domain of a homogenous system that can be described by coherent rotation [see Eq. (3)]. However, the small defects do take a role by pinning the domain walls [see Eq. (5)]. It is likely that the reversal nuclei and the domain walls may be established at the defects by the thermal activation. Only when the reversal field reaches the switching field can the domain wall be moved. Otherwise, the magnetization vector in every domain can only rotate coherently. By doing so, we really considered the role of the defects and the thermal activation by catching their essence, instead of their details. This is why our simple model can well describe the experimental results.

The two-path reversal model of coercivity unites the unpinning model and the nucleation model by relaxing some limitations on both models. If appropriate limitations are set to the two-path model, it reduces to either the unpinning or the nucleation model. Thus the two-path model can better describe the whole hysteresis loop measured at any orientation referred to the easy direction. Even for the simple case of single-crystal Fe films, Florczak and Dahlberg[6] found that fitting the coherent rotation model to the experimental hysteresis loops could not reconstruct simultaneously the experimental values of the switching fields and the saturation field. On the other hand, although the domain-wall unpinning model can explain the ''two jumps'' [7] and even the ''three jumps'' [8] in a hysteresis loop of single-crystal Fe films if the jumps are at small fields, this model cannot explain the switching behavior at high fields.

The two-path reversal mechanism was observed in (001)-oriented single-crystal Fe films with fourfold in-plane anisotropy by domain observation,[5] and here it was extended to apply to hard/soft exchange-coupled NiFe/SmFe/NiFe trilayers with well-defined uniaxial anisotropy. This implies that the two-path model may be appropriate for permanent magnets with well-defined anisotropy, such as $Nd_2Fe_{14}B$ and $Sm_2Co_{17}B$. For the NiFe/SmFe/NiFe trilayers, when the external field is along the easy axis, the magnetization reversal is caused by domain-wall unpinning. When the external field is along or near the hard axis, the magnetization reversal is caused by coherent rotation. In the other cases, the magnetization first rotates gradually by the coherent rotation and then sharply switches by domain-wall unpinning. If the same conclusions are applicable to permanent magnets with well-defined anisotropy, it is easy to understand why neither the pinning model nor the nucleation model can well describe the dependence of the coercivity on the angle between the external field and the easy axis. In contrast to this, the poor agreement in the angular dependence of the coercivity be-

tween theoretical predictions and experimental results, according to the viewpoint of Kronmüller *et al.*, is attributed to misaligned grains, local stray fields, and reduced anisotropy in grain boundaries.[1]

Since the macromagnetic properties of the exchange-coupled trilayers directly depend on the thickness of each layer, this provides another variable for studying the mechanism of coercivity. By comparison, single films and magnetic bulk materials do not have this advantage, so the mechanism of magnetic reversal in these systems is often studied by measuring the temperature dependence and the angle dependence of the coercivity.[1,19,20] On the other hand, this also presents a challenge to all theoretical models. A good model should at least be able to describe the thickness dependence of the coercivity. As for Eq. (2), it is essentially the coherent rotation approximation, and it reduces to the nucleation field of a single film if either $t_h=0$ or $t_s=0$ is set. Thus it is too simple to quantitatively describe the coercivity of hard/soft exchange-coupled multilayers. By contrast, the two-path reversal model gives a good description of the dependence of the coercivity on the thickness of NiFe layers.

Furthermore, in the two-path model, the pinning energy density $\varepsilon(H)$ takes a critical role, but it cannot be known in advance within the model itself. In order to gain a more fundamental understanding of magnetic reversal, it is necessary to carry out a micromagnetic calculation based on the physical picture of the two-path reversal model.

## V. CONCLUSIONS

The magnetic-reversal mechanism of $Ni_{80}Fe_{20}/Sm_{40}Fe_{60}/Ni_{80}Fe_{20}$ trilayers with in-plane uniaxial anisotropy was experimentally and theoretically studied by measuring and fitting the hysteresis loops. Our theoretical model of magnetic reversal unites the coherent rotation and domain-wall unpinning by relaxing some limitations on both models. Different processes of magnetic reversal were found by fitting the model to the experimental hysteresis loops. The magnetization reversal is caused by domain-wall unpinning when the external field is along the easy axis. When the external field is along or near the hard axis, the magnetization reversal is caused by coherent rotation. In the other cases (universal cases), the magnetization first rotates gradually by the coherent rotation and then sharply switches by domain-wall unpinning. Moreover, it was found that the domain-wall angle and the pinning energy at the sharp switching strongly depend on the angle between the external field and the easy axis. Furthermore, the dependence of the easy-axis coercivity on the thickness of $Ni_{80}Fe_{20}$ layers was theoretically reproduced by an extended model of domain-wall unpinning.

## ACKNOWLEDGMENTS

This work was supported by NSF-DMR-9713497, and we acknowledge the use of MRSEC shared facilities (NSF-DMR-9809423).

*Corresponding author. FAX: (205)348-2346. Email address: syan@mint.ua.edu

[1] H. Kronmüller, K.-D. Durst, and M. Sagawa, J. Magn. Magn. Mater. **74**, 291 (1988).
[2] R. Friedberg and D. I. Paul, Phys. Rev. Lett. **34**, 1234 (1975).
[3] D. I. Paul, J. Appl. Phys. **53**, 1649 (1982).
[4] A. Sakuma, S. Tanigawa, and M. Tokunaga, J. Magn. Magn. Mater. **84**, 52 (1990).
[5] Shi-shen Yan, R. Schreiber, P. Grünberg, and R. Schäfer, J. Magn. Magn. Mater. **210**, 309 (2000).
[6] J. M. Florczak and E. Dan Dahlberg, Phys. Rev. B **44**, 9338 (1991).
[7] R. P. Cowburn, S. J. Gray, J. Ferré, J. A. C. Bland, and J. Miltat, J. Appl. Phys. **78**, 7210 (1995).
[8] R. P. Cowburn, S. J. Gray, and J. A. C. Bland, Phys. Rev. Lett. **79**, 4018 (1997).
[9] R. Skomski and J. M. D. Coey, Phys. Rev. B **48**, 15 812 (1993).
[10] R. Skomski, J. Appl. Phys. **76**, 7059 (1994).
[11] E. Quandt and A. Ludwig, J. Appl. Phys. **85**, 6232 (1999).
[12] Eric E. Fullerton, J. S. Jiang, M. Grimsditch, C. H. Sowers, and S. D. Bader, Phys. Rev. B **58**, 12 193 (1998).
[13] I. A. Al-omari and D. J. Sellmyer, Phys. Rev. B **52**, 3441 (1995).
[14] M. Shindo, M. Ishizone, H. Kato, T. Miyazaki, and A. Sakuma, J. Magn. Magn. Mater. **161**, 1 (1996).
[15] E. Goto, N. Hayashi, T. Miyashita, and K. Nakagawa, J. Appl. Phys. **36**, 2951 (1965).
[16] S. Mangin, A. Sulpice, G. Marchal, C. Bellouard, W. Wernsdorfer, and B. Barbara, Phys. Rev. B **60**, 1204 (1999).
[17] K. Mibu, T. Nagahama, T. Shinjo, and T. Ono, Phys. Rev. B **58**, 6442 (1998).
[18] F. Y. Yang, C. L. Chen, E. F. Ferrari, X. W. Li, Gang Xiao, and A. Gupta, Appl. Phys. Lett. **77**, 286 (2000).
[19] D. Elbaz, D. Givord, S. Hirosawa, F. P. Missell, M. F. Rossignol, and V. Villas-boas, J. Appl. Phys. **69**, 5492 (1991).
[20] D. Givord, P. Tenaud, and T. Viadieu, J. Magn. Magn. Mater. **72**, 247 (1988).